Chapter 2
An Investigation of Complex Mode Shapes

C. Verhoeven, D. J. Ewins, M. H. M. Ellenbroek, X. Yao, and D. Di Maio

Abstract This paper presents an investigation of complex mode shape analysis caused by non-linear damping. Nowadays, most academics are accustomed to complex mode shapes, which are a characteristic of most axisymmetric structures. The topic was deeply investigated during the 1980s, sparking the sharpest debates about their physical existence or not. However, after nearly three decades, one question still stands, do we know all about complex mode shapes? This paper takes the dust off this topic again and explores how complex eigenvectors arise when the percentage frequency separation between two mode shapes is the same order of magnitude as the percentage damping. The difference between the past and present investigations relates to the non-linear damping that might arise from joint dynamics under various vibration amplitudes. Hence, the new research question is about the investigation of amplitude-dependent damping on the modal complexity. Why bother? There are several engineering applications in both space and aerospace where axisymmetric structures and joint dynamics can impair the numerical analysis that is currently performed. This paper does not offer any solutions but does expand the research on an unsolved challenge by identifying the questions posed.

Keywords Complex modes · Non-proportional damping · Non-linear · MSC · MCF

2.1 Introduction

Mathematically a mode shape is defined as a manifestation of eigenvectors that describe the relative displacement of two or more elements in a mechanical system. These mode shapes are real if these elements move through the equilibrium at the same time. If this is not the case, the mode shapes are considered to be complex. The existence of complex mode shapes has been known for several decades. Research on this topic has been conducted, but not as much compared to other fields within structural dynamics. Possible reasons for this are the fact that highly complex modes do not often occur, with the exception of axisymmetric structures. Only when two natural frequencies are close and the system contains non-proportional damping can highly complex modes occur [1].

In practice, when analysing a structure using a finite element method, the damping is often not included in detail but may be represented by simple proportional damping. This latter case means that the eigenvectors will all be real. This is an issue if the experimental analysis has complex eigenvectors due to the fact that in reality there is non-proportional damping.

C. Verhoeven · M. H. M. Ellenbroek
Department of Applied Mechanics, Mechanical Engineering, University of Twente, Enschede, Netherlands
e-mail: c.verhoeven@student.utwente.nl; m.ellenbroek@airbusDS.nl

D. J. Ewins
Imperial College London, London, UK
e-mail: d.ewins@imperial.ac.uk

X. Yao
Department of Applied Mechanics, Mechanical Engineering, University of Twente, Enschede, Netherlands

School of Aviation Engineering, Civil Aviation Flight University of China, Deyang, China
e-mail: yaoxingyu@buaa.edu.cn

D. Di Maio (✉)
Department of Applied Mechanics, Mechanical Engineering, University of Twente, Enschede, Netherlands

Department of Mechanical Engineering, University of Bristol, Bristol, UK
e-mail: d.dimaio@utwente.nl

M. R. W. Brake et al. (eds.), *Nonlinear Structures & Systems, Volume 1*, Conference Proceedings of the Society for Experimental Mechanics Series, https://doi.org/10.1007/978-3-031-04086-3_2

This non-proportionality can have many sources, e.g. bolted connections or added dampers at specific locations. To make comparison between the FE model and the experimental possible, the complex mode shapes are converted to real mode shapes. F. Buffe et al. [2] introduced non-proportional damping, and thus complexity, into the FE model which increased the accuracy of the simulation.

It appears that often complex modes are considered an undesirable complication rather than as a blessing. However some attempts have been made to make use of complex mode shapes. E. Lofrano et al. [3] proposed a method to detect damage. One basic assumption is that damage results in a local increase of damping making the damping matrix non-proportional and thus resulting in complex mode shapes. Detecting this complexity in the mode shapes provides information about the damage done to system.

The layout of this paper is as follows. First an overview of the methods used will be given. After that, a simple model will be used to show the requirements for complex mode shapes. Four cases are discussed, proportional and non-proportional damping for separated modes and close modes. The modal parameters are calculated as well as multiple quantifiers for complexity. Finally the importance of the location of the non-proportional damping will be discussed. It will also be shown that the non-linear damper results in a complex operating deflection shape.

2.2 Methodology

Modal analysis allows us to obtain the linear normal mode shapes corresponding to the natural frequencies [1]. This paper uses this theory to obtain and investigate both real and complex mode shapes. Different types of damping exist which require different analytical approaches to solve. The first part of this paper is based around a system containing structural damping. Classical structural damping is chosen which depends on the displacements. This means there are no velocity terms in the equation of motion (EOM) which makes solving it easier. The EOM of a structural damped system is as follows:

$$[\mathbf{M}]\,\ddot{\mathbf{x}}\,(\mathbf{t}) + [\mathbf{K} + \mathbf{iD}]\,\boldsymbol{x}\,(\boldsymbol{t}) = \boldsymbol{f}\,(\boldsymbol{t}) \tag{2.1}$$

where **[M]** is the mass matrix, **[K]** the stiffness matrix and **[D]** the structural damping matrix which are all of size 4×4. $\ddot{\boldsymbol{x}}\,(\boldsymbol{t})$ is the acceleration vector of the DOFS, $\boldsymbol{x}(\boldsymbol{t})$ the displacement vector and $\boldsymbol{f}(\boldsymbol{t})$ the force vector which are all 4×1 in size.

Eigenvalues and eigenvectors can be computed by solving the eigenvalue problem:

$$[\mathbf{M}]\,\boldsymbol{\lambda}^{\mathbf{2}}\Psi = +\,[\mathbf{K} + \mathbf{iD}]\,\Psi \tag{2.2}$$

where the eigenvectors Ψ represent the unscaled mode shapes and the eigenvalues represent the natural frequencies and loss factor [4]:

$$\boldsymbol{\lambda}_{\mathbf{n}}^{\mathbf{2}} = \boldsymbol{\omega}_{\mathbf{n}}^{\mathbf{2}}\left(\mathbf{1} + \mathbf{i}\boldsymbol{\eta}_{\mathbf{n}}\right) \tag{2.3}$$

Besides the standard modal constants, three complexity quantifiers are used. Imregun and Ewins ([5]) have defined multiple parameters, called modal complexity factors (MCF), to quantify the amount of complexity in a system. MCF I focusses on the difference between the phases of the eigenvector components. MCF II takes into account the magnitude of the eigenvectors as well as their phase angles. Figure 2.1 shows how the MCF II is computed in a 4 DOF system.

The final quantifier for complexity is called the mode shape complexity (MSC) [6]. This parameter is based on the strain energy of the system and can be calculated as follows:

$$MSC_n = \frac{\min\,(U_n)}{\max\,(U_n)} \tag{2.4}$$

where U_n is the strain energy during an oscillation of mode n.

A switch will be made from structural damping to viscous damping for investigating the effect of non-linearity. This switch is necessary since quadratic structural damping does not exist. The EOM of the viscous non-linear model is as follows:

$$[\mathbf{M}]\,\ddot{\mathbf{x}}\,(\mathbf{t}) + [\mathbf{C}]\,\dot{\mathbf{x}}\,(\mathbf{t}) + [\mathbf{C_{NL}}]\,\mathrm{sign}\,(\dot{\mathbf{x}}\,(\mathbf{t}))\,\dot{\mathbf{x}}(\mathbf{t})^{\mathbf{2}} + [\mathbf{K}]\,\mathbf{x}\,(\mathbf{t}) = \mathbf{f}\,(\mathbf{t}) \tag{2.5}$$

where $[\boldsymbol{C}_{\mathbf{NL}}]$ is build up using the damping constant(s) of the non-linear damper.

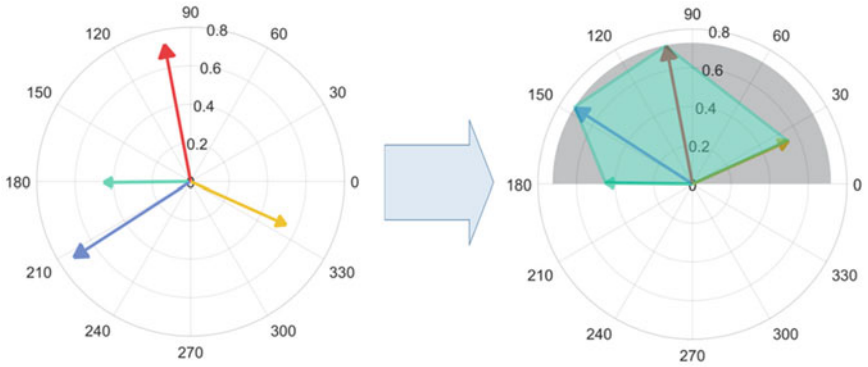

Fig. 2.1 The MCF II is the area spanned by the eigenvector tips divided by the area of half a circle, where the radius of this circle is equal to the magnitude of the largest eigenvector

The equation will be solved using time integration. To achieve this the EOM has to be transformed to the state space:

$$\begin{bmatrix} \dot{\mathbf{x}} \\ \ddot{\mathbf{x}} \end{bmatrix} = \begin{bmatrix} 0 & 1 & 0 \\ -\mathbf{M}^{-1}\mathbf{K} & -\mathbf{M}^{-1}\mathbf{C} & -\mathbf{M}^{-1}\mathbf{C_{NL}} \bullet \text{sign}(\dot{\mathbf{x}}) \end{bmatrix} \begin{bmatrix} \mathbf{x} \\ \dot{\mathbf{x}} \\ \dot{\mathbf{x}}^2 \end{bmatrix} + \begin{bmatrix} \mathbf{0} \\ -\mathbf{M}^{-1} \end{bmatrix} \mathbf{f} \tag{2.6}$$

The Runga-Kutta time integration scheme can now be used to find the numerical solution.

2.3 Structural Damped MDOF System

A MDOF spring damper system has been created with the purpose of exploring complex mode shapes. This system contains 4 masses and 7 springs and dampers and can be seen in Fig. 2.2. The masses are assumed to move only in horizontal direction which makes this a 4 DOF system. In the first part of this paper, the damping is defined as structural damping instead of the more conventional viscous damping. The advantage of structural damping is that it is easier to model. The EOM looks as follows:

$$[\boldsymbol{M}]\,\ddot{\boldsymbol{x}}\,(\boldsymbol{t}) + [\boldsymbol{K} + \boldsymbol{Di}]\,\boldsymbol{x}\,(\boldsymbol{t}) = \boldsymbol{f}\,(\boldsymbol{t}) \tag{2.7}$$

where:

$$[\boldsymbol{M}] = \text{diag}\,(m_1, m_2, m_3, m_4)$$

$$[\boldsymbol{K}] = \begin{bmatrix} \boldsymbol{k_1 + k_2 + k_3} & \boldsymbol{-k_2} & \boldsymbol{-k_3} & \boldsymbol{0} \\ & \boldsymbol{k_2 + k_4} & \boldsymbol{0} & \boldsymbol{-k_4} \\ & \textbf{sym.} & \boldsymbol{k_3 + k_5 + k_6} & \boldsymbol{-k_5} \\ & & & \boldsymbol{k_4 + k_5 + k_7} \end{bmatrix}$$

$$[\boldsymbol{D}] = \begin{bmatrix} \boldsymbol{d_1 + d_2 + d_3} & \boldsymbol{-d_2} & \boldsymbol{-d_3} & \boldsymbol{0} \\ & \boldsymbol{d_2 + d_4} & \boldsymbol{0} & \boldsymbol{-d_4} \\ & \textbf{sym.} & \boldsymbol{d_3 + d_5 + d_6} & \boldsymbol{-d_5} \\ & & & \boldsymbol{d_4 + d_5 + d_7} \end{bmatrix}$$

The vector $\boldsymbol{x}$ contains the displacements of the masses. The dot ($\dot{}$) indicates that the time derivative of the variable is taken. The force vector $\boldsymbol{f(t)}$ is 0 since we are interested in the free vibration response. The values chosen for the masses are $m_1 = 1,\ m_3 = 2.7,\ m_4 = 4$ kg. The stiffness constants are $k_1 = k_3 = k_4 = k_5 = k_7 = 10^6, k_2 = 1.82 \bullet 10^6, k_6 = 0.7 \bullet 10^6$ N/m. m_2 and the damping values are not defined, since these will change throughout this paper. One might wonder why k_2 and k_6 have such specific stiffness values. The reason for this is that with these stiffness values it is possible to get the natural

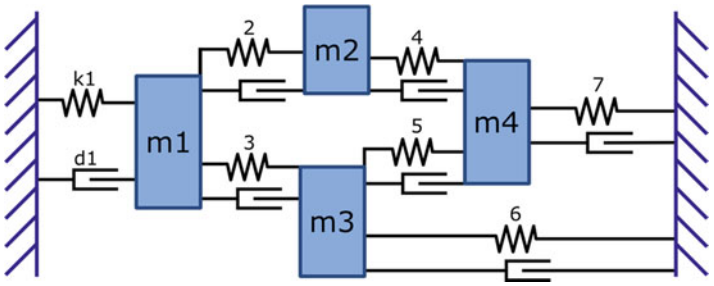

Fig. 2.2 MDOF spring damper system

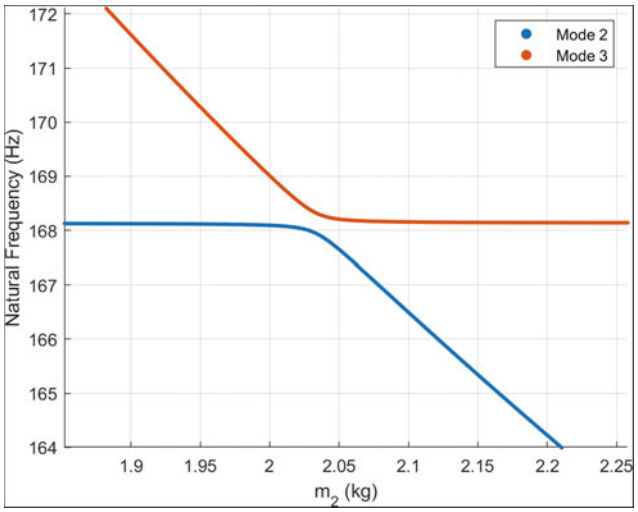

Fig. 2.3 Effect of m_2 on natural frequency 2 and 3, undamped system

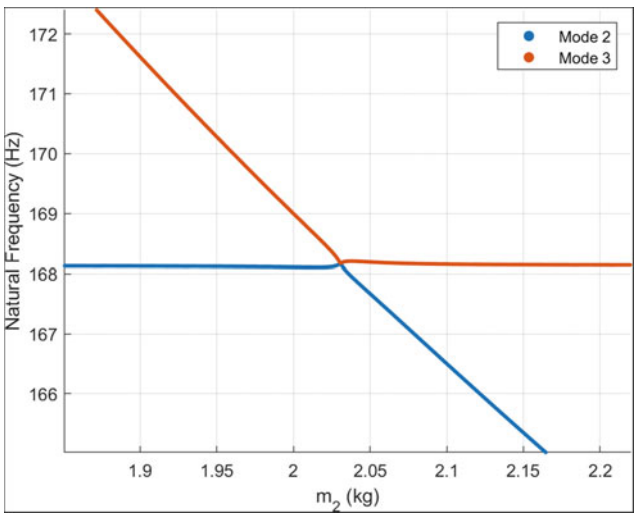

Fig. 2.4 Effect of m_2 on natural frequency 2 and 3, damped system

frequencies of mode 2 and 3 close by adjusting m_2 (see Fig. 2.3). For specific damping values, it is even possible to make the natural frequencies of mode 2 and 3 intersect (see Fig. 2.4).

The undamped receptance frequency response function (FRF) for this system when $m_2 = 2.6$ kg can be seen in Fig. 2.5. The four resonance frequencies can be clearly observed. The choice has been made to show only the response of mass 3.

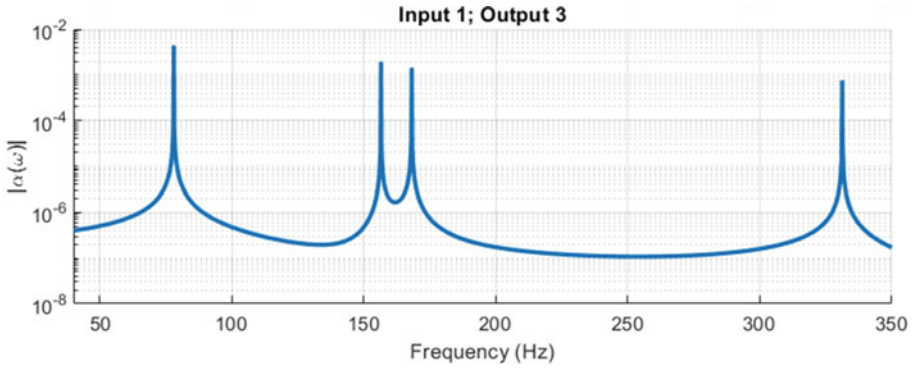

Fig. 2.5 Undamped forced response of mass 3

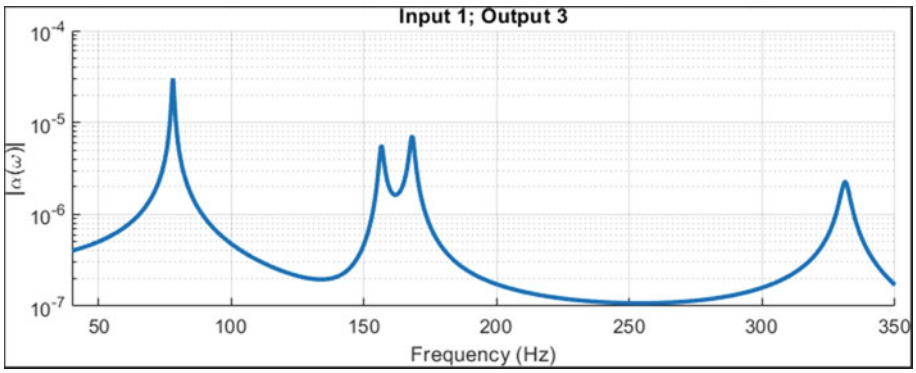

Fig. 2.6 Force response of mass 3, case I

2.3.1 Case I: Proportional Damping, Separated Modes

A damped system is either proportionally damped or non-proportionally damped. The system is proportionally damped if the damping matrix is a linear combination of the mass and stiffness matrices: $[\boldsymbol{D}] = \boldsymbol{\alpha}[\boldsymbol{M}] + \boldsymbol{\beta}[\boldsymbol{K}]$, where $\boldsymbol{\alpha}$ and $\boldsymbol{\beta}$ can have any constant value. In the 4 DOF system, the damping values are chosen in such a way that $[\boldsymbol{D}] = \mathbf{0.01}[\boldsymbol{K}]$, meaning that the system is proportionally damped. Mass 2 has a weight of 2.6 kg. The FRF of mass 3 can be seen in Fig. 2.6. It is clear that the peaks are less sharp compared to the undamped case.

Solving the eigenvalue problem of this system results in the eigenvalues and eigenvectors. These eigenvalues and eigenvectors provide information about the resonance frequencies, damping and mode shapes of the system. The mode shapes can be seen in Fig. 2.7. The normalized eigenvectors can be seen in Fig. 2.8. The colours of the arrows correspond to the colours of the masses in Fig. 2.7. Note that the eigenvectors are completely real meaning that the phase difference between de DOFs is either 0°or 180°.

2.3.2 Case II: Non-proportional Damping, Separated Modes

Non-proportionally damped systems are very common in practice. Non-proportional damping can have many different causes, e.g. hinges, damage to the structure and shock absorbers. To create a non-proportionally damped system in this study, the damping values are changed. They are defined as follows:

$$[d_1 \;\; d_2 \;\; d_3 \;\; d_4 \;\; d_5 \;\; d_6 \;\; d_7] = 10^{-2} \cdot \left[\tfrac{1}{2}k_1 \;\; 3k_2 \;\; \tfrac{1}{2}k_3 \;\; \tfrac{3}{2}k_4 \;\; \tfrac{1}{2}k_5 \;\; \tfrac{3}{2}k_6 \;\; \tfrac{1}{2}k_7 \right]$$

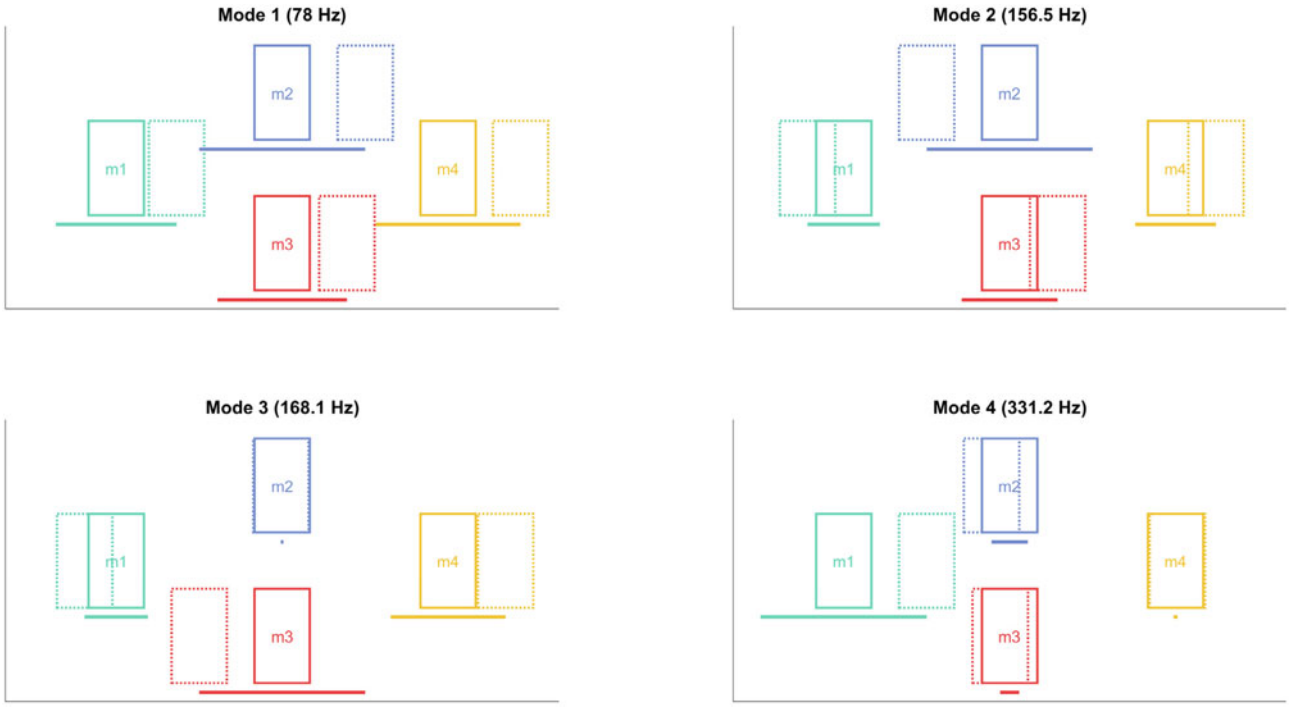

Fig. 2.7 Mode shapes of the proportionally damped system

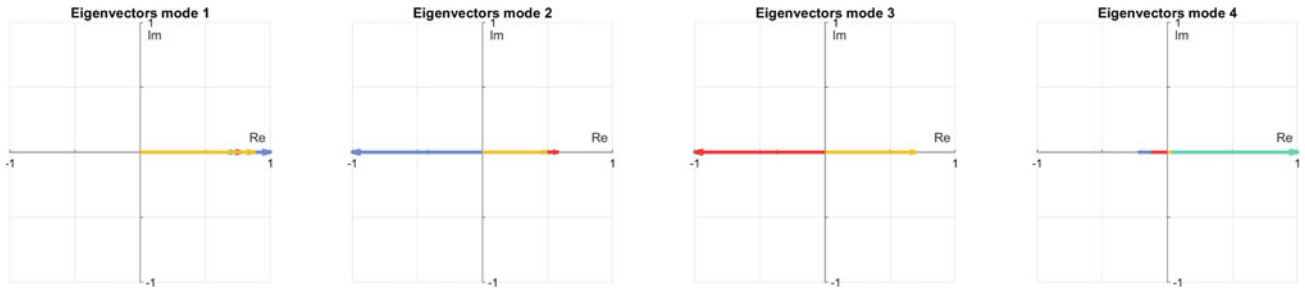

Fig. 2.8 Eigenvectors proportionally damped system

These values where obtained by trial and error. There are many more damping values which will result in highly complex mode shapes. Using these damping values results in the following eigenvectors (visualized in Fig. 2.9):

$$\Psi_1 = \begin{bmatrix} 0.720 + 0.002i \\ 0.991 - 0.009i \\ 0.773 - 0.005i \\ 0.866 + 0.004i \end{bmatrix} \quad \Psi_2 = \begin{bmatrix} -0.364 + 0.065i \\ -0.830 + 0.170i \\ 0.479 - 0.101i \\ 0.405 - 0.081i \end{bmatrix} \quad \Psi_3 = \begin{bmatrix} -0.315 - 0.061i \\ -0.013 + 0.000i \\ -0.824 - 0.176i \\ 0.573 + 0.118i \end{bmatrix} \quad \Psi_4 = \begin{bmatrix} 0.999 - 0.001i \\ -0.218 - 0.003i \\ -0.114 + 0.002i \\ 0.023 + 0.000i \end{bmatrix}$$

The difference between proportionally and non-proportionally damped systems is that the eigenvectors of the non-proportionally damped system contain complex terms. These complex terms indicate a phase offset of the DOFs. The angle of the eigenvector with respect to the positive real axis in the Argand diagram describes the phase angle (see Fig. 2.9). So if the eigenvector contains complex terms, the phase angle is not 0°or 180°. This means that when observing the mode shapes of the system, the masses do generally not cross the equilibrium simultaneously which is known as a travelling wave.

An important question that arises is how to quantify the amount of complexity in each mode shape. For this paper the choice is made to utilize the MCF I, MCF II and MSC. The higher the percentage, the more complex the system is. Table 2.1 shows the properties of the non-proportionally damped system with separated modes (Fig. 2.10).

Fig. 2.9 Eigenvectors of the non-proportional damped system with separated modes

Table 2.1 Properties of a non-proportionally damped system

Mode #	ω (Hz)	η	Complexity (%)		
			MCF I	MCF II	MSC
1	78	0.008	0	0	0
2	157	0.014	1	8	0
3	168	0.008	6	9	0
4	331	0.018	1	0	0

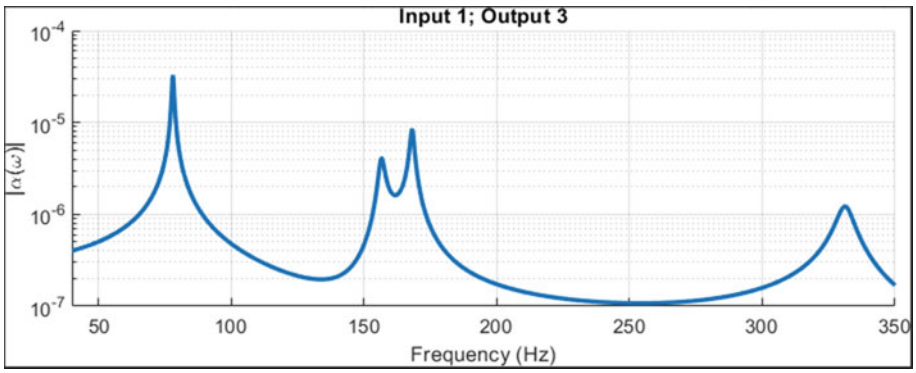

Fig. 2.10 FRF case II

2.3.3 *Discussion About the Validity of MCF II*

One might be surprised by the fact that the MCF II for mode 2 and 3 are relatively high although the eigenvectors appear to be mostly in line with each other. This is caused by how the MCF II is calculated. Reference [5] suggested that first all eigenvectors should be converted to the [0°,180°] region, by making the imaginary part of the eigenvectors positive. If one then computes the area covered by the tips of the eigenvectors, the area can be quite large even if the eigenvectors were in line with each other. This is especially the case if the eigenvectors are under an angle of 45°and − 135°. One could argue that a system in which the eigenvectors are in line with each other should not be considered complex, since the masses pass the equilibrium simultaneously. It is up to the reader to decide how trustworthy the complexity quantifiers are.

2.3.4 *Case III: Proportional Damping, Close Modes*

So far we have seen that, for proportionally damped systems, the eigenvectors are completely real and for non-proportional damped system the eigenvectors contain small complex parts. However in both situations, the modes were well separated ($\Delta\omega_n > 10$). Mode 2 and 3 can be brought closer by changing mass 2 from 2.6 kg to 2.037 kg. Figure 2.11 shows the eigenvectors of the proportionally damped system. It is clear that all the eigenvectors are still real, meaning the mode shape is a standing wave. Even for higher levels of damping, when the loss factor (η) is 1, the eigenvectors are still completely real. One might start to wonder if it is mathematically possible that the eigenvectors contain an imaginary component if the damping is proportional. It is actually possible for very specific settings that complexity will occur in the eigenvector. However the vectors will still be exactly 0 or 180° apart (Fig. 2.12).

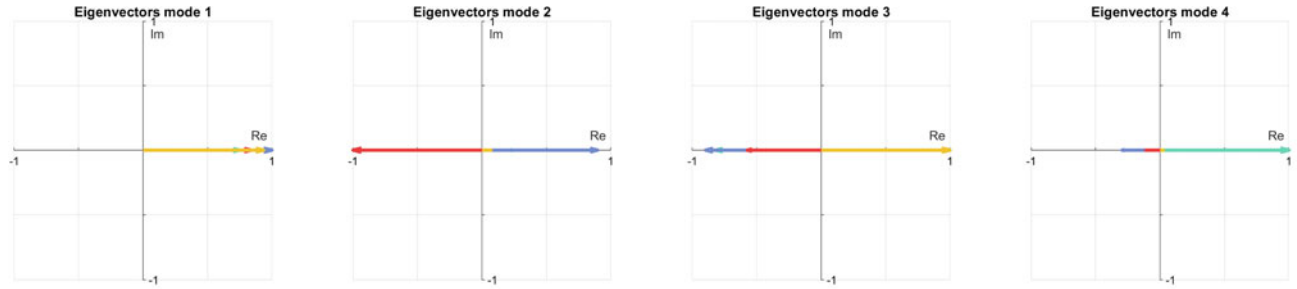

Fig. 2.11 Eigenvectors of the proportional damped system when mode 2 and 3 are close

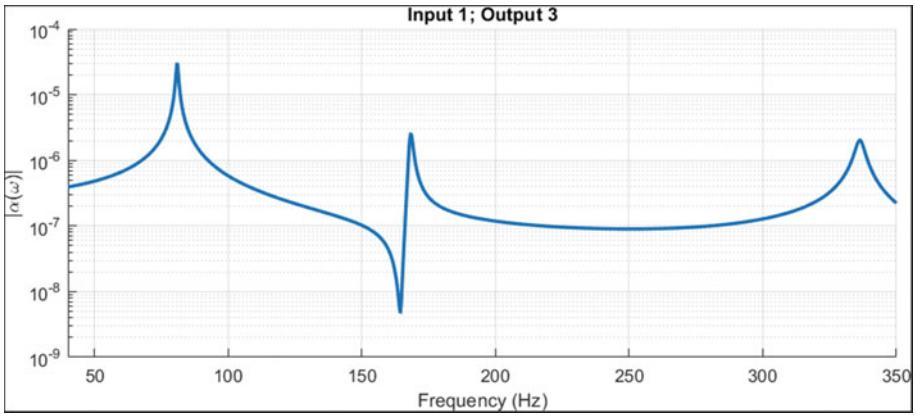

Fig. 2.12 FRF case III

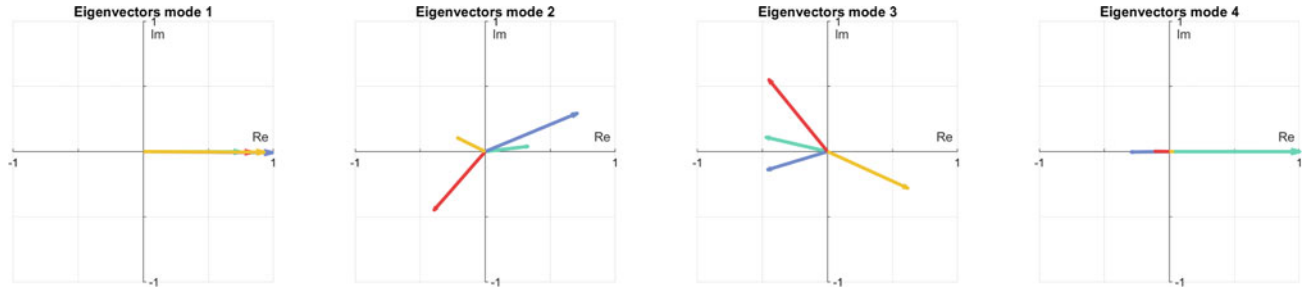

Fig. 2.13 Eigenvectors of the non-proportional damped system when mode 2 and 3 are close

2.3.5 Case IV: Non-proportional Damping, Close Modes

For the non-proportionally damped system, the eigenvectors contain large imaginary components as can be seen in Fig. 2.13. This shows that for mode 2 and 3 the motion of the individual masses is out of phase with respect to each other. This complexity can also be seen when looking at the modal complexity factors in Table 2.2 and Fig. 2.14.

2.3.6 Effect of the Closeness of the Natural Frequencies on the Complexity

In the previous section, it is shown that the non-proportional damping will result in complex modes. However, the importance of two of the system's natural frequencies being close for generating complex modes is not yet clear. Adjusting mass 2 changes the closeness of the natural frequencies of mode 2 and 3. This will be used to obtain more insight in how the closeness of the natural frequencies influences the complexity. At a mass of 2.00058 kg, the natural frequencies are equal. The mass can be lowered or raised to increase the difference between natural frequencies of mode 2 and 3. Figure 2.15 shows

Table 2.2 Properties of damped systems with close modes

Damping	Mode #	ω (Hz)	η	Complexity (%)		
				MCF I	MCF II	MSC
Proportional	1	81	0.01	0	0	0
	2	167.9	0.01	0	0	0
	3	168.3	0.01	0	0	0
	4	336	0.01	0	0	0
Non-proportional	1	81	0.009	0	0	0
	2	168.0	0.013	50	30	13
	3	168.2	0.009	38	42	13
	4	336	0.019	1	0	0

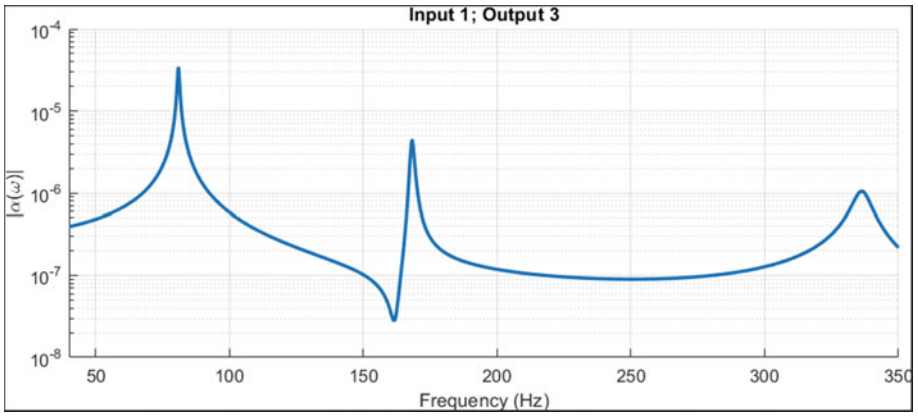

Fig. 2.14 FRF case IV

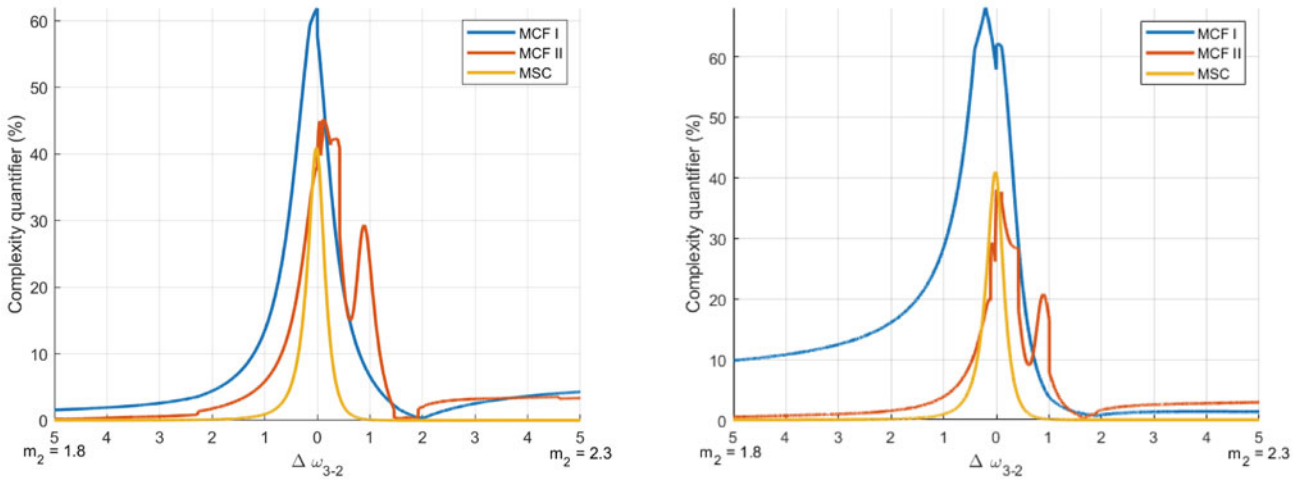

Fig. 2.15 MCFs and MSC as a function of $\Delta\omega_{3-2}(m_2)$. (a) Mode 2. (b) Mode 3

the MCFs and MSC when mass 2 (m_2) and thus the difference between ω_3 and ω_2 changes. For the MCFs it is difficult to find clear patterns, but in general, MCF I and MCF II become smaller when the natural frequencies get further apart. The MSC, on the other hand, shows a distinct bell shape. The MSC shows a maximum when the natural frequencies are 0.017 Hz apart. What is also interesting to observe is that the MSC curve is equal (difference $<<1\%$) for mode 2 and 3. Although the ratio between the maximum and minimum strain energy of mode 2 and 3 is equal, the strain energy of mode 2 is not the same as that of mode 3 (Fig. 2.16).

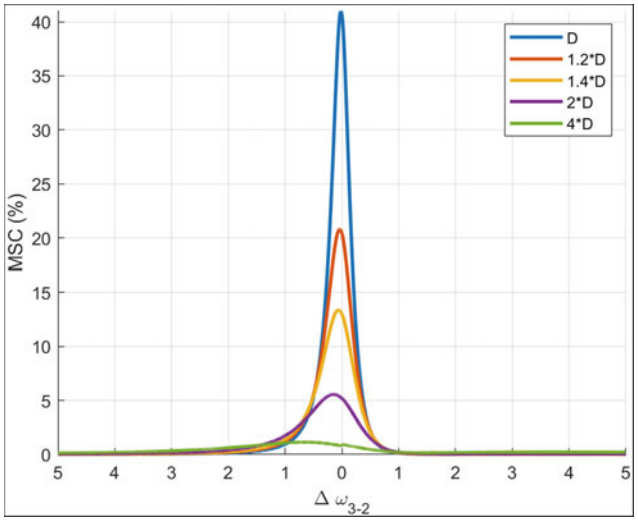

Fig. 2.16 Effect of m_2 on the MSC for different damping values

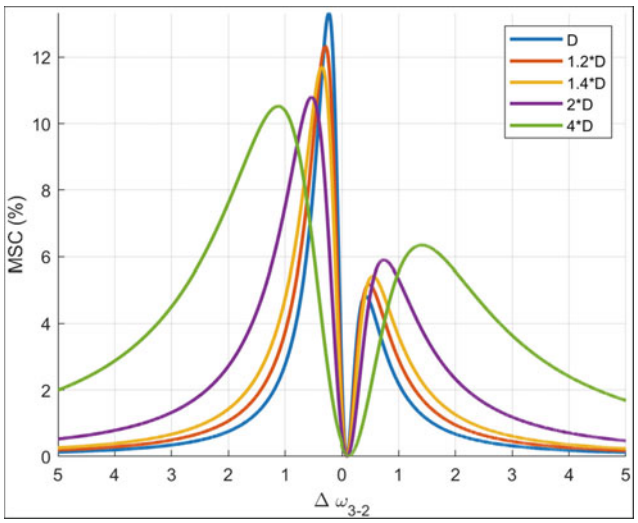

Fig. 2.17 Effect of m_4 on the MSC for different damping values

The MSC is chosen to compare the effect of different damping levels. The non-proportional damping matrix is multiplied with different factors to observe the influence of the damping amplitude on the MSC. For each different damping setting, the MSC values were computed for a range of m_2 values, which controls the closeness between ω_3 and ω_2. The results can be seen in Fig. 2.17. It can be observed that a low damping results in a high narrow bell shape. Increasing the damping flattens out this bell shape. Furthermore the peak tends to move slightly to the left when the damping is increased. One might wonder if the peak would reach 100% if the damping would be lowered. Unfortunately for this case, lowering the damping prevents the crossing of the natural frequencies from mode 2 and 3. Another question is if this bell shape behaviour always looks like in Fig. 2.17. The answer is no. If one tunes $\Delta\omega 3{-}2$ by changing m_4 instead of m_2, the bell curves look different (see Fig. 2.17). Instead of one peak around $\Delta\omega 3{-}2 = 0$, there are two peaks, one at each side. These peaks also differ in height.

2.4 Effect of Non-linear Damper Location

From this section onwards, the structural damping will be replaced by viscous damping. Time integration is used to calculate the behaviour of the system.

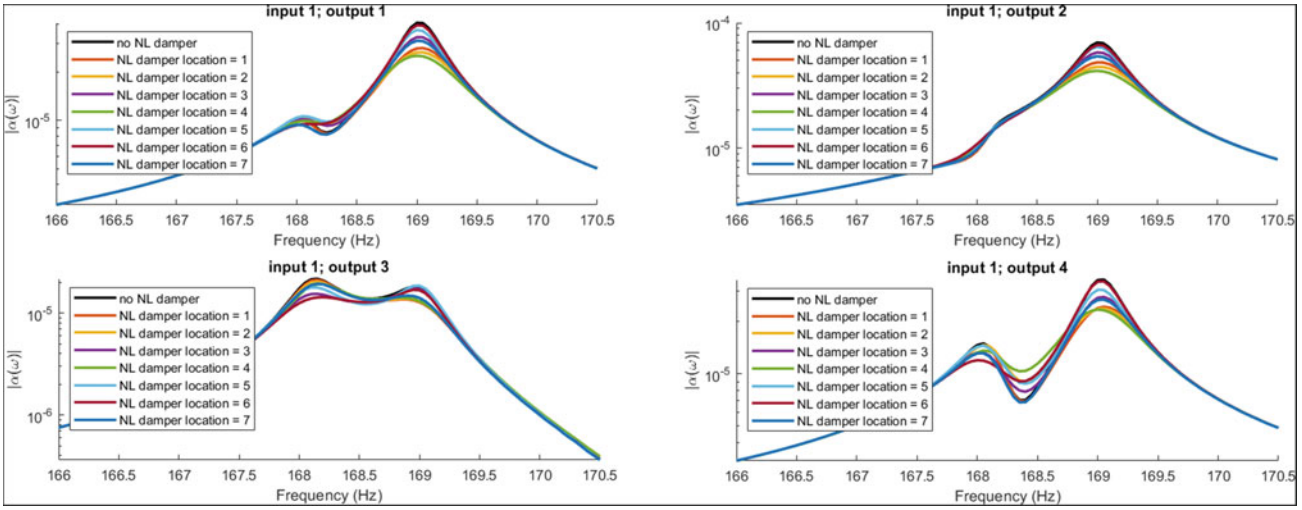

Fig. 2.18 FRF for different locations of the non-linear damper

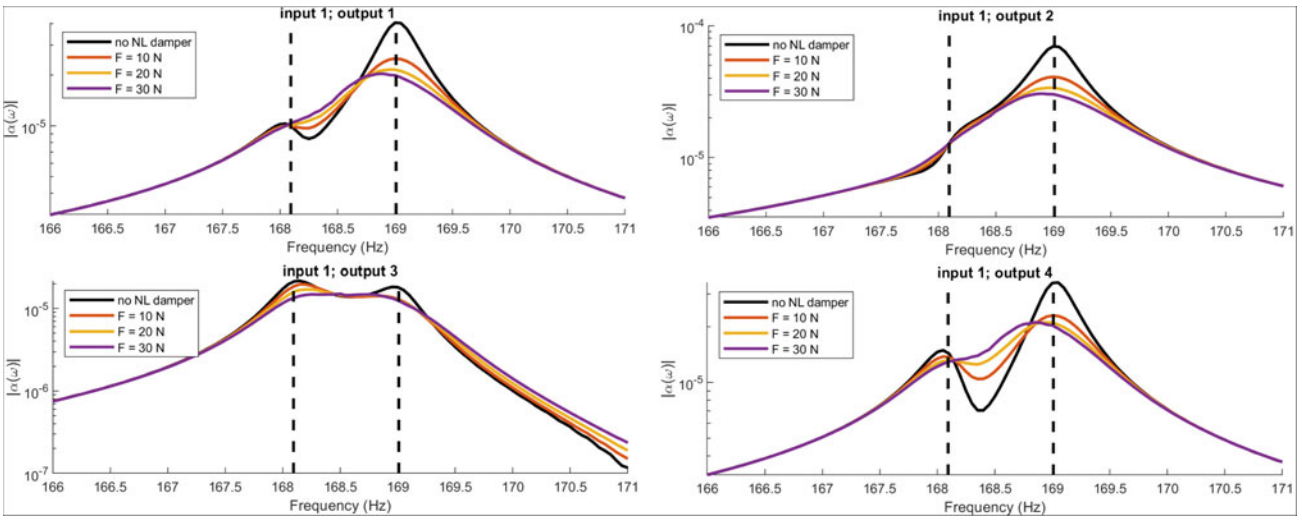

Fig. 2.19 FRF for different force amplitudes. The vertical lines represent the natural frequencies of the undamped system

To determine if the location of a NL damper has a significant effect, a quadratic NL damper is added. The location if this NL damper changes from position 1 till 7. The damping constant is 40 N/m^{2}s^{-2} for the NL damper and 2 m/s for the linear dampers. The amplitude of the harmonic excitation force is 10 N. For each of the seven setups, the FRFs are calculated. Figure 2.18 shows the FRF for different locations of the NL damper. It clearly shows that the location of the NL damper is of importance. When using a sine sweep with a range of 50 till 300 Hz as excitation profile, the energy dissipated by the NL damper is 16 times higher when this damper is located at location 2 instead of location 6.

2.5 Complexity Due to Non-linear Damping

A NL damper with a damping constant of 40 N/m^{2}s^{-2} is placed at location 4. The other dampers have a damping constant such that $\mathbf{[D]} = 10^{-6}\mathbf{[K]}$, meaning that the non-proportionality in the damping is a result of the NL damper.

In Fig. 2.19 it can be observed how two separated peaks merge when the force increases and a NL damper is present. Since the system is non-linear, there are no linear normal modes. However, one can observe the operating deflection shape (ODS). Figure 2.20 shows the ODS of the system at the undamped natural frequencies for mode 2 and 3. It is clear that the behaviour is complex. Figure 2.21 shows the ODS of the system when there is no NL damping but only proportional

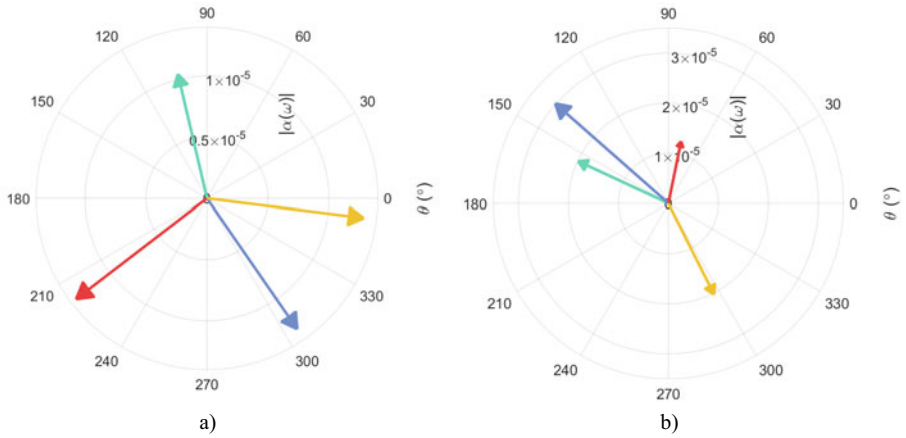

a) b)

Fig. 2.20 ODS for different excitation frequencies. The system contains a NL damper as is described in this section. The angle θ reprents the phase difference between the excitation and the movement of the mass. The length of the arrows represents the magnitude of the motion. (**a**) 168.1 Hz. (**b**) 169 Hz

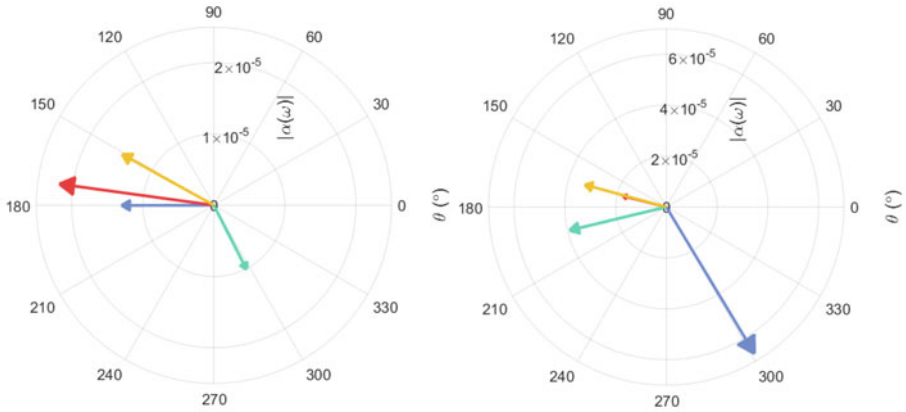

a) b)

Fig. 2.21 ODS for the system without a NL damper, meaning the system is proportionally damped. (**a**) 168.1 Hz. (**b**) 169 Hz

damping. One might expect the system to show no complex behaviour; however it can be seen that there is also complexity when the system is proportionally damped. Even though the mode shapes are real, the ODS is still complex since both close modes have an influence on the ODS. If the natural frequencies would be far apart, the ODS would be almost completely described by a single mode, and thus it would not be complex.

2.6 Conclusion and Future Work

The requirements for complex modes have been explored using a theoretical 4 DOF spring-damper system. This study confirms that proportional damping is impossible to obtain complex modes. Highly complex modes can be achieved if the damping is non-proportional and the natural frequencies are close. Using the MSC it has been shown that the optimal frequency difference of two close modes depends on the damping, the mass and possibly more parameters. This paper mainly focused on the basis of complex mode shapes. An unanswered question is whether or not the presence of complex mode shapes has an effect on the damping. Experimental research will be required to answer this question.

References

1. Ewins, D.J.: Modal Testing: Theory, Practice and Application, 2nd edn. Research Studies Press, London (2000)
2. F. Buffe et al.: A complex mode approach for the validation of FE models with structural damping (2014)
3. Lofrano, E., Paolone, A., Ruta, G.: Dynamic damage identification using complex mode shapes. Struct. Control. Health Monit. **27** (Sept. 2020). https://doi.org/10.1002/stc.2632
4. He, J., Fu, Z.-F.: 6 – Modal analysis of a damped MDoF system. In: He, J., Fu, Z.-F.. (eds.) Modal Analysis, pp. 123–139. Oxford: Butterworth-Heinemann, (2001). isbn: 978-0-7506-5079-3. https://doi.org/10.1016/B978-075065079-3/50006-1
5. Imregun, Ewins, D.J.: Complex modes-origins and limits, pp. 496–504 (1995)
6. Koruk, H., Sanliturk, K.Y.: A novel definition for quantification of mode shape complexity. J. Sound Vib. **332**(14), 3390–3403 (2013). issn: 0022-460X. https://doi.org/10.1016/j.jsv.2013.01.039